

Imino–Rhodium(III) and –Ruthenium(II) Compounds with Stereogenic Metal Centers

Daniel Carmona,* Cristina Vega, Fernando J. Lahoz, Sergio Elipe, and Luis A. Oro

Departamento de Química Inorgánica, Instituto de Ciencia de Materiales de Aragón, Universidad de Zaragoza-Consejo Superior de Investigaciones Científicas, 50009 Zaragoza, Spain

M. Pilar Lamata, Fernando Viguri, and Ricardo García-Correas

Departamento de Química Inorgánica, Escuela Universitaria de Ingeniería Técnica Industrial, Instituto de Ciencia de Materiales de Aragón, Universidad de Zaragoza-Consejo Superior de Investigaciones Científicas, Corona de Aragón 35, 50009 Zaragoza, Spain

Carlos Cativiela* and M. Pilar López-Ram de VÍu

Departamento de Química Orgánica, Instituto de Ciencia de Materiales de Aragón, Universidad de Zaragoza-Consejo Superior de Investigaciones Científicas, 50009 Zaragoza, Spain

Received December 28, 1998

The synthesis and characterization of optically active imino complexes (R_M or S_M)-[(η^5 -C₅Me₅)RhCl(imine)][SbF₆] (imine = L_n = *N*-(2-pyridylmethylene)-(*R*)-1-phenylethylamine (L₁) (**1a,a'**), *N*-(2-pyridylmethylene)-(*R*)-1-naphthylethylamine (L₂) (**2a,a'**), *N*-(2-pyridylmethylene)-(*R*)-1-cyclohexylethylamine (L₃) (**3a,a'**) or [(η^6 -*p*-MeC₆H₄ⁱPr)RuCl(imine)]A (A = SbF₆, imine = L₁ (**4a,a'**), L₂ (**5a,a'**), L₃ (**6a,a'**), *N*-(2-pyridylmethylene)-(*1R,2S,4R*)-1-bornylamine (L₄) (**7a,a'**); A = BF₄, imine = L₁ (**4b,b'**), L₂ (**5b,b'**), L₃ (**6b,b'**), L₄ (**7b,b'**)) is reported. The absolute crystal structures of the (R_{Rh})-**1a** and (R_{Ru})-**7b** epimers were determined by X-ray analysis. Both complexes possess a chiral metal center in a pseudo-octahedral environment, being bonded to an η^5 -C₅Me₅ group (**1a**) or to an (η^6 -*p*-MeC₆H₄ⁱPr) ring (**7b**), a terminal chloride, and, in a chelating fashion, to the two nitrogen atoms of the imine ligand. At room temperature, in acetone or chloroform, the complexes are configurationally stable but in refluxing methanol epimerize at the metal center. Dichloromethane/acetone solutions of the solvate complexes [(η^n -ring)M(imine)S]²⁺ are active catalysts for the Diels–Alder reaction between methacrolein or acrolein and cyclopentadiene. The reaction occurs rapidly at room temperature and, in general, good exo/endo selectivities and moderate enantioselectivities are achieved.

Introduction

The use of optically active organometallic compounds in the stoichiometric or catalytic enantioselective synthesis of chiral organic compounds has increased enormously in the past few years.¹ In particular, transition metal complexes with stereogenic metal centers are especially useful for stereochemical studies which can allow us to obtain a better understanding of the stereocontrol of the enantioselectivity.² Most of these complexes possess half-sandwich geometries containing, in some instances, chiral chelating ligands.³

Several (η^6 -arene)Ru complexes with optically active chelating imines have been previously reported, and the stereochemistry at the ruthenium and their chiroptical properties have been studied.⁴ However, as far as we

are aware, the only known half-sandwich imino–rhodium compound is the C₅Me₅ derivative [(η^5 -C₅Me₅)-RhCl]L (L = (*S*)-*N*-(1-phenylethyl)salicylaldiminate).⁵

Although chiral transition metal half-sandwich compounds have been extensively used as catalysts or catalyst precursors in various organic processes, the catalytic use of imino compounds of this type has been very scarce. As far as we know, only the asymmetric

(1) (a) Brunner, H.; Zettlmeier, W. *Handbook of Enantioselective Catalysis*; VCH: Weinheim, Germany, 1993. (b) *Catalytic Asymmetric Synthesis*; Ojima, I., Ed.; VCH: Weinheim, Germany, 1993. (c) Noyori, R. *Asymmetric Catalysis in Organic Synthesis*; John Wiley and Sons: New York, 1994.

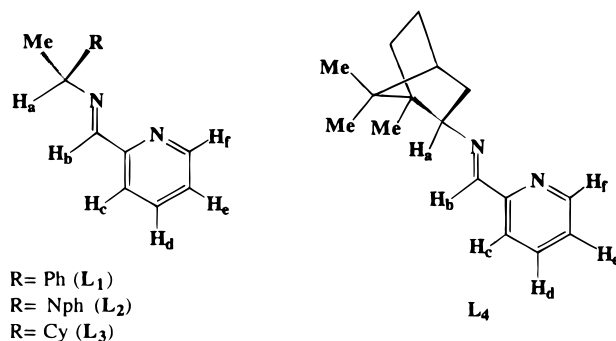
(2) (a) Organometallic Compounds and Optical Activity. *J. Organomet. Chem.* **1989**, *370*. (b) Meyer, O.; Arif, A. M.; Gladysz, J. A. *Organometallics* **1995**, *14*, 1844 and references therein. (c) Johnson, T. J.; Alvey, L. J.; Brady, M.; Mayne, C. L.; Arif, A. M.; Gladysz, J. A. *Chem.–Eur. J.* **1995**, *1*, 294 and references therein. (d) Consiglio, G.; Morandini, F. *Chem. Rev.* **1987**, *87*, 761. (e) Brookhardt, M.; Timmers, D.; Tucker, J. R.; Williams, G. D.; Husk, G. R.; Brunner, H.; Hammer, B. *J. Am. Chem. Soc.* **1983**, *105*, 6721. (f) Sokolov, V. I. *Chirality and Optical Activity in Organometallic Compounds*; Gordon and Breach Science Publishers: New York, 1990. (g) Morrison, J. D., Ed. *Asymmetric Synthesis*; Academic Press: Orlando, 1985; Vol. 5. (h) Bosnich, B., Ed. *Asymmetric Catalysis*; Martinus Nijhoff Publishers: Dordrecht, The Netherlands, 1986. (i) Davies, S. G. *Pure Appl. Chem.* **1988**, *60*, 40. (j) Davies, S. G. *Aldrichimica Acta* **1990**, *23*, 31. (k) Faller, J. W.; Chase, K. J. *Organometallics* **1995**, *14*, 1592.

hydrogen transfer reduction of alkyl–aryl ketones with 2-propanol, catalyzed by ruthenium complexes generated in situ from $[(\eta^6\text{-C}_6\text{H}_6)\text{RuCl}]_2(\mu\text{-Cl})_2$ and chiral Schiff bases derived from (1*R*,2*R*)-diaminocyclohexane and aromatic aldehydes, has previously been reported.⁶

We are interested in the preparation, characterization, stereochemical properties, and catalytic applications of d⁶ pseudotetrahedral compounds with chiral chelating ligands such as α -amino acidates,⁷ (*R*)-1,2-bis-(diphenylphosphino)propane,^{3c,d} phosphino oxazolines,^{3m} or chiral imines.⁸ In particular, we have recently shown the ability of imino–iridium(III) cations of formula $[(\eta^5\text{-C}_5\text{Me}_5)\text{IrCl}(\text{L}_n)]^+$ (L_n represents an enantiopure chiral imine ligand derived from 2-pyridinecarbaldehyde) to act as catalyst precursors for the Diels–Alder reaction between methacrolein and cyclopentadiene.⁸

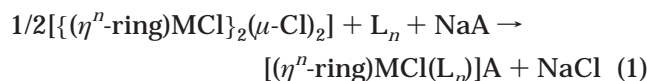
In the present paper, we describe the synthesis and characterization of complexes containing the fragments $(\eta^6\text{-}p\text{-MeC}_6\text{H}_4\text{iPr})\text{Ru}$ and $(\eta^5\text{-C}_5\text{Me}_5)\text{Rh}$ of general formula $[(\eta^n\text{-ring})\text{MCl}(\text{L}_n)]\text{A}$ with enantiopure chiral imine ligands ($\text{L}_n = \text{L}_1\text{--L}_4$, Scheme 1; $\text{A} = \text{SbF}_6$ or BF_4). The absolute configuration at the metal is assigned by a combination of X-ray diffraction, circular dichroism, and NMR spectroscopic measurements. We have also studied the conformational and configurational stability of the new compounds and their use as enantioselective catalyst precursors for the Diels–Alder reaction between acrolein or methacrolein and cyclopentadiene.

Scheme 1



Results and Discussion

Synthesis and Characterization of the Complexes 1–7. At room temperature, the dimers $[(\eta^n\text{-ring})\text{MCl}]_2(\mu\text{-Cl})_2$ ($(\eta^n\text{-ring})\text{M} = (\eta^5\text{-C}_5\text{Me}_5)\text{Rh}^9$ or $(\eta^6\text{-}p\text{-MeC}_6\text{H}_4\text{iPr})\text{Ru}^{10}$) react, in methanol, with stoichiometric amounts of the corresponding imine $\text{L}_1\text{--L}_4$ (Scheme 1) and NaA ($\text{A} = \text{SbF}_6$ or BF_4) to give, in 74–94% chemical yield, diastereomeric mixtures of $[(\eta^n\text{-ring})\text{MCl}(\text{L}_n)]\text{A}$ which differ in their configuration at the stereogenic metal center (eq 1).



complex	$(\eta^n\text{-ring})\text{M}$	L_n	A	a/a' or b/b' molar ratio
1a,a'	$(\eta^5\text{-C}_5\text{Me}_5)\text{Rh}$	L_1	SbF_6	94:6
2a,a'	$(\eta^5\text{-C}_5\text{Me}_5)\text{Rh}$	L_2	SbF_6	55:45
3a,a'	$(\eta^5\text{-C}_5\text{Me}_5)\text{Rh}$	L_3	SbF_6	41:59
4a,a'	$(\eta^6\text{-}p\text{-MeC}_6\text{H}_4\text{iPr})\text{Ru}$	L_1	SbF_6	65:35
4b,b'	$(\eta^6\text{-}p\text{-MeC}_6\text{H}_4\text{iPr})\text{Ru}$	L_1	BF_4	65:35
5a,a'	$(\eta^6\text{-}p\text{-MeC}_6\text{H}_4\text{iPr})\text{Ru}$	L_2	SbF_6	63:37
5b,b'	$(\eta^6\text{-}p\text{-MeC}_6\text{H}_4\text{iPr})\text{Ru}$	L_2	BF_4	58:42
6a,a'	$(\eta^6\text{-}p\text{-MeC}_6\text{H}_4\text{iPr})\text{Ru}$	L_3	SbF_6	42:58
6b,b'	$(\eta^6\text{-}p\text{-MeC}_6\text{H}_4\text{iPr})\text{Ru}$	L_3	BF_4	42:58
7a,a'	$(\eta^6\text{-}p\text{-MeC}_6\text{H}_4\text{iPr})\text{Ru}$	L_4	SbF_6	44:56
7b,b'	$(\eta^6\text{-}p\text{-MeC}_6\text{H}_4\text{iPr})\text{Ru}$	L_4	BF_4	52:48

Complexes **1–7** have been characterized by IR and NMR spectroscopy, elemental analysis, and the X-ray crystal structure determination of compounds **1a** and **7b**. Their IR spectra show a band at ca. 1600 cm^{-1} which can be assigned to the $\nu(\text{C}=\text{N})$ vibration of the imine ligand. Table 1 collects the ^1H NMR spectroscopic data for these complexes. In all cases, these data were consistent with the presence of the η^n -ring and the pyridine–imine ligands in a 1:1 ratio. The isomer ratio was obtained from accurate integration¹¹ of the H_a or the deshielded H_b imino proton signals of each diastereomer (Scheme 1). Due to the different solubility in methanol, it has proved possible to obtain diastereomeric mixtures with distinct compositions by fractional crystallization from this solvent. When the asymmetric imine carbon has an aromatic substituent (L_1 or L_2), there is a significant chemical shift difference between the iminic proton H_b of each pair of diastereomers (from 0.22 to 0.71 ppm; see Table 1). This observation, which

(9) White, C.; Yates A.; Maitlis, P. M. *Inorg. Synth.* **1992**, *29*, 228.

(10) Bennett, M. A.; Huang, T.-N.; Matheson, T. W.; Smith, A. K. *Inorg. Synth.* **1982**, *21*, 75.

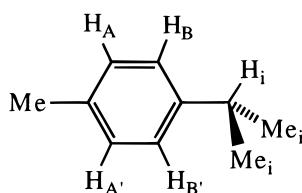
(11) Error limits on each integer are estimated as ± 2 .

- (3) Severin, K.; Berge, R.; Beck, W. *Angew. Chem., Int. Ed.* **1998**, *37*, 1634, and references therein. (b) Enders, D.; Gielen, H.; Raabe, G.; Runsink, J.; Teles, J. H. *Chem. Ber.* **1997**, *130*, 1253. (c) Carmona, D.; Lahoz, F. J.; Oro, L. A.; Lamata, M. P.; Viguri, F.; San José, E. *Organometallics* **1996**, *15*, 2961. (d) Carmona, D.; Cativiela, C.; García-Correas, R.; Lahoz, F. J.; Lamata, M. P.; López, J. A.; López-Ram de Viú, M. P.; Oro, L. A.; San José, E.; Viguri, F. *J. Chem. Soc., Chem. Commun.* **1996**, 1247. (e) Attar, S.; Nelson, J. H.; Fischer, J.; de Cian, A.; Sutter, J.-P.; Pfeffer, M. *Organometallics* **1995**, *14*, 4559. (f) Attar, S.; Catalano, V. J.; Nelson, J. H. *Organometallics* **1996**, *15*, 2932. (g) Hapiot, F.; Agbossou, F.; Meliet, C.; Mortreux, A.; Rosair, G. M.; Welch, A. J. *New J. Chem.* **1997**, *21*, 1161. (h) Hashiguchi, S.; Fujii, A.; Takehara, J.; Ikariya, T.; Noyori, R. *J. Am. Chem. Soc.* **1995**, *117*, 7562. (i) Uematsu, N.; Fujii, A.; Hashiguchi, S.; Ikariya, T.; Noyori, R. *J. Am. Chem. Soc.* **1996**, *118*, 4916. (j) Haak, K.-J.; Hashiguchi, S.; Fujii, A.; Ikariya, T.; Noyori, R. *Angew. Chem., Int. Ed. Engl.* **1997**, *36*, 285. (k) Hashiguchi, S.; Fujii, A.; Haak, K.-J.; Matsumura, K.; Ikariya, T.; Noyori, R. *Angew. Chem., Int. Ed. Engl.* **1997**, *36*, 288. (l) Zanetti, N. C.; Spindler, F.; Spencer, J.; Togni, A.; Rihs, G. *Organometallics* **1996**, *15*, 860. (m) Carmona, D.; Cativiela, C.; Elipse, S.; Lahoz, F. J.; Lamata, M. P.; López-Ram de Viú, M. P.; Oro, L. A.; Vega, C.; Viguri, F. *J. Chem. Soc., Chem. Commun.* **1997**, 2351. (n) Davies, D. L.; Fawcett, J.; Garratt, S. A.; Russell, D. R. *J. Chem. Soc., Chem. Commun.* **1997**, 1351. (o) Davenport, A. J.; Davies, D. L.; Fawcett, J.; Garratt, S. A.; Latesh, L.; Russell, D. R. *J. Chem. Soc., Chem. Commun.* **1997**, 2347. (4) (a) Mandal, S. K.; Chakravarty, A. R. *J. Organomet. Chem.* **1991**, *417*, C59. (b) Mandal, S. K.; Chakravarty, A. R. *J. Chem. Soc., Dalton Trans.* **1992**, 1627. (c) Mandal, S. K.; Chakravarty, A. R. *Inorg. Chem.* **1993**, *32*, 3851. (d) Brunner, H.; Oeschey, R.; Nuber, B. *Angew. Chem., Int. Ed. Engl.* **1994**, *33*, 866. (e) Brunner, H.; Oeschey, R.; Nuber, B. *Inorg. Chem.* **1995**, *34*, 3349. (f) Brunner, H.; Oeschey, R.; Nuber, B. *Organometallics* **1996**, *15*, 3616 and references therein. (g) Brunner, H.; Oeschey, R.; Nuber, B. *J. Organomet. Chem.* **1996**, *518*, 47. (h) Brunner, H.; Oeschey, R.; Nuber, B. *J. Chem. Soc., Dalton Trans.* **1996**, 1499. (i) Davies, D. L.; Fawcett, J.; Krafczyk, R.; Russell, D. R. *J. Organomet. Chem.* **1997**, *545/546*, 581. (5) Loza, M. L.; Parr, J.; Slawin, A. M. Z. *Polyhedron* **1997**, *16*, 2321. (6) Krasik, P.; Alper, H. *Tetrahedron* **1994**, *50*, 4347. (7) (a) Carmona, D.; Mendoza, A.; Lahoz, F. J.; Oro, L. A.; Lamata, M. P.; San José, E. *J. Organomet. Chem.* **1990**, *396*, C17. (b) Carmona, D.; Lahoz, F. J.; Atencio, R.; Oro, L. A.; Lamata, M. P.; San José, E. *Tetrahedron: Asymmetry* **1993**, *4*, 1425. (c) Jimeno, M. L.; Elguero, J.; Carmona, D.; Lamata, M. P.; San José, E. *Magn. Reson. Chem.* **1996**, *34*, 42. (d) Lamata, M. P.; San José, E.; Carmona, D.; Lahoz, F. J.; Atencio, R.; Oro, L. A. *Organometallics* **1996**, *15*, 4852. (8) Carmona, D.; Lahoz, F. J.; Elipse, S.; Oro, L. A.; Lamata, M. P.; Viguri, F.; Mir, C.; Cativiela, C.; López-Ram de Viú, M. P. *Organometallics* **1998**, *17*, 2986.

Table 1. ^1H NMR Spectroscopic Data^{a,b} for Complexes 1–7

complex	C_5Me_5	Me	H_a	H_b	others	
1a	1.83 (s)	1.88 (d, $J_{\text{HaH}} = 7.0$)	5.78 (qd, $J_{\text{HaHb}} = 1.1$)	8.40 (dd, $J_{\text{RhHb}} = 2.9$)	8.16 (m, H_c), 8.28 (m, H_d), 7.94 (m, H_e), 9.12 (d, $J_{\text{HeHf}} = 5.5$, H_f), 7.4–7.6 (m, Ph)	
1a'	1.82 (s)		5.62 (m)	9.11 (s)	9.00 (H_f)	
2a	1.82 (s)	2.08 (d, $J_{\text{HaH}} = 6.7$)	6.43 (q)	8.54 (bs)	9.19 (d, $J_{\text{HeHf}} = 5.3$, H_f), 7.4–8.5 (m, H_{c-e} , Ph)	
2a'	1.73 (s)	2.13 (d, $J_{\text{HaH}} = 6.6$)	6.66 (q)	9.24 (bs)	9.11 (d, $J_{\text{HeHf}} = 5.1$, H_f), 7.4–8.5 (m, H_{c-e} , Ph)	
3a	1.81 (s)	1.48 (d, $J_{\text{HaH}} = 6.6$)	4.19 (m)	8.89 (d, $J_{\text{RhHb}} = 2.7$)	8.21 (m, H_c), 8.29 (m, H_d), 7.91 (m, H_e), 9.08 (d, $J_{\text{HeHf}} = 5.1$, H_f), 1.1–2.2 (m, Cy)	
3a'	1.79 (s)	1.52 (d, $J_{\text{HaH}} = 6.6$)	4.58 (m)	8.73 (bs)	8.23 (m, H_c), 8.29 (m, H_d), 7.92 (m, H_e), 9.03 (d, $J_{\text{HeHf}} = 5.4$, H_f), 0.8–2.4 (m, Cy)	
complex	<i>p</i> -Cymene			imine		
4a	0.93 (d, $J_{\text{HH}} = 7.0$, Me _i), 2.28 (s, Me), 2.95 (psp, CH _i), 5.60, 6.23 ($J_{\text{AB}} = 5.9$, H_AH_B), 5.70, 5.88 ($J_{\text{A'B'}} = 6.6$, H_AH_B)	1.08 (d, $J_{\text{HH}} = 6.6$, Me _i)		1.88 (d, $J_{\text{HaH}} = 6.9$, Me), 5.97 (q, H_a), 7.4–7.6 (m, Ph), 7.71 (m, H_e), 7.85 (m, H_d), 8.30 (bs, H_c), 8.84 (s, H_b), 9.61 (d, $J_{\text{HeHf}} = 5.7$, H_f)		
4a'	2.20 (s, Me)			2.02 (Me), 7.4–7.9 (m, H_{c-e} , Ph), 9.07 (s, H_b), 9.59 (H_f)		
4b	0.91 (d, $J_{\text{HH}} = 6.6$, Me _i), 2.26 (s, Me), 2.54 (psp, CH _i), 5.57, 6.24 ($J_{\text{AB}} = 6.0$, H_AH_B), 5.67, 5.87 ($J_{\text{A'B'}} = 6.1$, H_AH_B)	1.06 (d, $J_{\text{HH}} = 6.8$, Me _i)		1.87 (d, $J_{\text{HaH}} = 6.8$, Me), 5.98 (q, H_a), 7.4–7.6 (m, Ph), 7.72 (m, H_e), 7.83 (bs, H_d), 8.30 (bs, H_c), 8.86 (s, H_b), 9.60 (d, $J_{\text{HeHf}} = 5.7$, H_f)		
4b'	0.89 (d, $J_{\text{HH}} = 7.0$, Me _i), 2.18 (s, Me), 2.54 (psp, CH _i)	1.06 (d, $J_{\text{HH}} = 7.3$, Me _i)		2.01 (d, $J_{\text{HaH}} = 6.8$, Me), 7.4–7.6 (m, Ph), 7.72 (m, H_e), 7.83 (bs, H_d), 8.30 (bs, H_c), 9.08 (s, H_b), 9.58 (H_f)		
5a	0.94 (d, $J_{\text{HH}} = 6.8$, Me _i), 2.26 (s, Me), 2.63 (psp, CH _i), 5.5–6.1 (H_AH_B , H_AH_B)	1.10 (d, $J_{\text{HH}} = 7.0$, Me _i)		1.32 (d, $J_{\text{HaH}} = 6.8$, Me), 6.67 (dq, H_a), 7.5–8.3 (m, H_d , H_e , Nph), 8.30 (d, $J_{\text{HdHc}} = 7.8$, H_c), 8.78 (d, $J_{\text{HaHb}} = 1.3$, H_b), 9.63 (d, $J_{\text{HeHf}} = 5.5$, H_f)		
5a'	0.78 (d, $J_{\text{HH}} = 7.0$, Me _i), 1.83 (s, Me), 2.37 (psp, CH _i), 5.4–6.1 (H_AH_B , H_AH_B)	0.81 (d, $J_{\text{HH}} = 6.8$, Me _i)		2.09 (d, $J_{\text{HaH}} = 6.6$, Me), 6.84 (q, H_a), 7.5–8.2 (m, H_d , H_e , Nph), 8.51 (d, $J_{\text{HdHc}} = 8.5$, H_c), 9.31 (s, H_b), 9.54 (d, $J_{\text{HeHf}} = 5.5$, H_f)		
5b	0.94 (d, $J_{\text{HH}} = 6.8$, Me _i), 2.26 (s, Me), 2.62 (psp, CH _i), 5.4–6.1 (H_AH_B , H_AH_B)	1.10 (d, $J_{\text{HH}} = 6.4$, Me _i)		6.68 (q, H_a), 7.7–8.4 (m, H_d , H_e , Nph), 8.14 (d, $J_{\text{HdHc}} = 7.5$, H_c), 8.81 (s, H_b), 9.65 (d, $J_{\text{HeHf}} = 5.2$, H_f)		
5b'	0.78 (d, $J_{\text{HH}} = 6.4$, Me _i), 1.82 (s, Me), 2.33 (psp, CH _i), 5.4–6.1	0.80 (d, $J_{\text{HH}} = 6.4$, Me _i)		6.85 (q, H_a), 7.5–8.1 (m, H_d , H_e , Nph), 8.55 (d, $J_{\text{HdHc}} = 8.3$, H_c), 9.33 (s, H_b), 9.56 (d, $J_{\text{HeHf}} = 5.3$, H_f)		
6a	1.05 (d, $J_{\text{HH}} = 7.0$, Me _i), 2.27 (s, Me), 5.8–6.3 (H_AH_B , H_AH_B)	1.20 (d, $J_{\text{HH}} = 6.8$, Me _i)		0.8–2.5 (m, Cy), 1.48 (d, $J_{\text{HaH}} = 6.7$, Me), 4.61 (m, H_a), 7.82 (m, H_e), 8.2–8.3 (m, H_c , H_d), 8.88 (s, H_b), 9.58 (H_f)		
6a'	1.03 (d, $J_{\text{HH}} = 7.0$, Me _i), 2.32 (s, Me), 2.81 (psp, CH _i), 5.8–6.3 (H_AH_B , H_AH_B)	1.18 (d, $J_{\text{HH}} = 7.0$, Me _i)		0.8–2.5 (m, Cy), 1.56 (d, $J_{\text{HaH}} = 6.7$, Me), 4.81 (m, H_a), 7.82 (m, H_e), 8.2–8.3 (m, H_c , H_d), 8.74 (s, H_b), 9.55 (d, $J_{\text{HeHf}} = 6.1$, H_f)		
6b	1.05 (d, $J_{\text{HH}} = 6.9$, Me _i), 2.27 (s, Me), 5.8–6.3 (H_AH_B , H_AH_B)	1.19 (d, $J_{\text{HH}} = 6.8$, Me _i)		0.8–2.5 (m, Cy), 1.48 (d, $J_{\text{HaH}} = 6.7$, Me), 4.59 (m, H_a), 7.82 (m, H_e), 8.2–8.3 (m, H_c , H_d), 8.88 (s, H_b), 9.58 (H_f)		
6b'	1.03 (d, $J_{\text{HH}} = 6.9$, Me _i), 2.31 (s, Me), 2.79 (psp, CH _i), 5.8–6.3 (H_AH_B , H_AH_B)	1.18 (d, $J_{\text{HH}} = 6.8$, Me _i)		0.8–2.5 (m, Cy), 1.55 (d, $J_{\text{HaH}} = 6.7$, Me), 4.81 (m, H_a), 7.82 (m, H_e), 8.2–8.3 (m, H_c , H_d), 8.74 (s, H_b), 9.56 (d, $J_{\text{HeHf}} = 6.4$, H_f)		
7a	1.05 (d, $J_{\text{HH}} = 6.8$, Me _i), 2.34 (s, Me), 2.72 (psp, H_i), 5.77, 6.34 ($J_{\text{AB}} = 6.8$, H_AH_B), 5.80, 6.32 ($J_{\text{A'B'}} = 6.6$, H_AH_B)	1.13 (d, $J_{\text{HH}} = 7.1$, Me _i)		0.96, 1.14, 1.37 (3xs), ^c 1.2–2.8 (m), ^d 5.36 (dd, $J_{\text{HHa}} = 10.5$, $J_{\text{HHa}} = 4.3$, H_a), 7.82, 8.28, 8.36 (ABX system, $J_{\text{AB}} = 6.8$, $J_{\text{BX}} = 7.7$, H_e , H_d , H_c), 8.92 (s, H_b), 9.50 (d, $J_{\text{HeHf}} = 5.5$, H_f)		
7a'	1.08 (d, $J_{\text{HH}} = 7.0$, Me _i), 2.31 (s, Me), 5.88, 6.25 ($J_{\text{AB}} = 6.1$, H_AH_B), 5.93, 6.18 ($J_{\text{A'B'}} = 6.2$, H_AH_B)	1.10 (d, $J_{\text{HH}} = 6.8$, Me _i)		0.94, 1.14, 1.32 (3xs), ^c 1.2–2.8 (m), ^d 4.99 (m, H_a), 7.82, 8.28, 8.42 (ABX system, $J_{\text{AB}} = 7.9$, $J_{\text{BX}} = 7.7$, H_e , H_d , H_c), 8.79 (d, $J_{\text{HaHb}} = 2.6$, H_b), 9.54 (d, $J_{\text{HeHf}} = 5.3$, H_f)		
7b	1.06 (d, $J_{\text{HH}} = 6.8$, Me _i), 2.35 (s, Me), 2.74 (psp, H_i), 5.78, 6.37 ($J_{\text{AB}} = 6.6$, H_AH_B), 5.82, 6.35 ($J_{\text{A'B'}} = 6.2$, H_AH_B)	1.14 (d, $J_{\text{HH}} = 6.8$, Me _i)		0.98, 1.20, 1.38 (3xs), ^c 1.3–2.7 (m), ^d 5.38 (dd, $J_{\text{HHa}} = 10.9$, $J_{\text{HHa}} = 4.3$, H_a), 7.83, 8.29, 8.38 (ABX system, $J_{\text{AB}} = 7.7$, $J_{\text{BX}} = 7.3$, H_e , H_d , H_c), 8.94 (s, H_b), 9.53 (d, $J_{\text{HeHf}} = 5.1$, H_f)		
7b'	1.08 (d, $J_{\text{HH}} = 6.9$, Me _i), 2.31 (s, Me), 2.79 (psp, H_i), 5.88, 6.26 ($J_{\text{AB}} = 5.9$, H_AH_B), 5.93, 6.21 ($J_{\text{A'B'}} = 6.2$, H_AH_B)	1.10 (d, $J_{\text{HH}} = 6.5$, Me _i)		0.94, 1.15, 1.33 (3xs), ^c 1.3–2.7 (m), ^d 5.01 (m, H_a), 7.83, 8.29, 8.42 (ABX system, $J_{\text{AB}} = 7.9$, $J_{\text{BX}} = 7.7$, H_e , H_d , H_c), 8.79 (d, $J_{\text{HaHb}} = 2.5$, H_b), 9.56 (d, $J_{\text{HeHf}} = 5.5$, H_f)		

^a Measured in $(\text{CD}_3)_2\text{CO}$. Chemical shifts in ppm from TMS as external standard. Coupling constants in hertz. Abbreviations: s, singlet; d, doublet; dd, doublet of doublets; pt, pseudotriplet; q, quartet; qd, quartet of doublets; psp, pseudoseptet; m, multiplet. ^b For imine protons labeling, see Scheme 1. For *p*-cymene protons labeling, see below. ^c Me groups of the bornyl substituent. ^d Remaining bornyl protons.



contains conformational and configurational information, will be discussed later.

Molecular Structure of the Diastereomers 1a and 7b. To determine the absolute configuration of the chloro-imino compounds the molecular structures of **1a**

and **7b** were elucidated by diffractometric means. Single crystals of the complexes were grown from spectroscopically enantiopure solutions of **1a** (^1H NMR, >98%) and from a 90:10 molar ratio mixture of compounds **7b/7b'**. Molecular representations of the cations of complexes

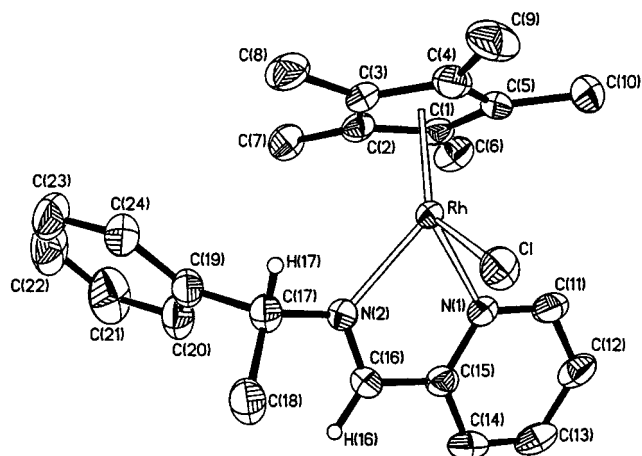


Figure 1. Molecular diagram of the R_{Rh} diastereoisomer of the cationic complex $[(\eta^5\text{-C}_5\text{Me}_5)\text{RhCl}(\text{L}_1)]^+$ (**1a**). Only two structurally significant hydrogens have been represented (H(16) and H(17)).

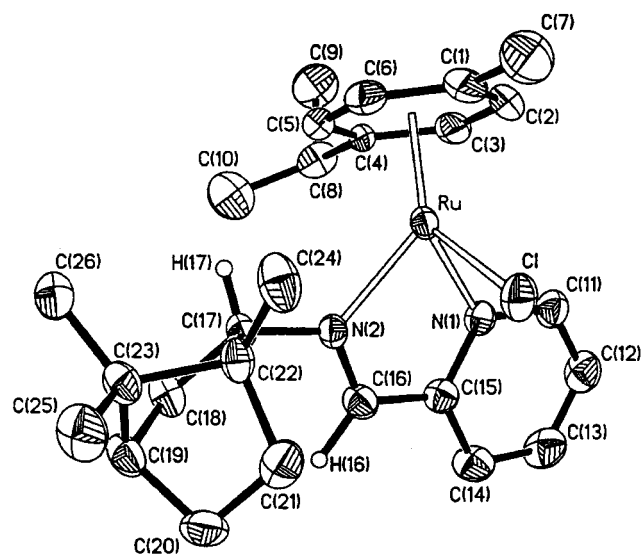


Figure 2. Molecular diagram of the R_{Ru} diastereoisomer of the cationic complex $[(\eta^6\text{-}p\text{-MeC}_6\text{H}_4\text{iPr})\text{RuCl}(\text{L}_4)]^+$ (**7b**). For clarity, only hydrogens H(16) and H(17) have been represented.

1a and **7b** are depicted in Figures 1 and 2, respectively, and selected structural parameters are listed in Table 2. Both cations exhibit distorted "three-legged piano stool" geometries. An $\eta^5\text{-C}_5\text{Me}_5$ (**1a**) or an $\eta^6\text{-}p\text{-MeC}_6\text{H}_4\text{iPr}$ (**7b**) group occupies three fac positions of an ideal metal-octahedral environment, and the chelate pyridine-imine ligand and a terminal chlorine atom complete the coordination sphere. In general, no significant differences are observed in the bond lengths and angles of the two structures with respect to those previously reported for imino- $(\eta^5\text{-C}_5\text{Me}_5)\text{Ir}^{\text{III}}$ or imino- $(\eta^6\text{-}p\text{-MeC}_6\text{H}_4\text{iPr})\text{Ru}^{\text{II}}$ compounds. The absolute configuration of the metal center is R for both complexes in accordance with the ligand priority sequence¹² $\eta^n\text{-ring} > \text{Cl} > \text{N}(\text{im}) > \text{N}(\text{py})$. In both structures, the $\text{Ir}(1)\text{-N}(1)\text{-C}(15)\text{-C}(16)\text{-N}(2)$ metallacycle is essentially planar. If both struc-

Table 2. Selected Bond Distances (Å) and Angles (deg) for Complexes **1a** and **7b**^a

	1a (M = Rh)	7b (M = Ru)
M-Cl	2.3845(13)	2.4040(14)
M-N(1)	2.113(4)	2.093(4)
M-N(2)	2.131(4)	2.127(4)
M-C(1)	2.159(4)	2.260(5)
M-C(2)	2.171(4)	2.219(5)
M-C(3)	2.167(4)	2.177(5)
M-C(4)	2.173(5)	2.236(5)
M-C(5)	2.154(4)	2.208(5)
M-C(6)		2.233(5)
M-G ^a	1.787(5)	1.705(5)
N(1)-C(11)	1.336(6)	1.351(6)
N(1)-C(15)	1.346(6)	1.352(6)
C(15)-C(16)	1.465(6)	1.470(7)
C(16)-N(2)	1.281(6)	1.295(6)
N(2)-C(17)	1.472(6)	1.498(6)
C(17)-C(18)	1.531(7)	1.588(7)
C(17)-C(19)/C(22)	1.521(6)	1.571(6)
Cl-M-N(1)	88.42(11)	82.08(11)
Cl-M-N(2)	83.15(10)	85.60(11)
Cl-M-G ^a	125.41(15)	128.13(18)
N(1)-M-N(2)	77.06(15)	77.28(14)
N(1)-M-G ^a	130.2(2)	131.0(2)
N(2)-M-G ^a	135.2(2)	133.7(2)
M-N(1)-C(11)	126.4(3)	125.8(3)
M-N(1)-C(15)	115.0(3)	115.5(4)
N(1)-C(15)-C(14)	122.5(4)	122.7(5)
N(1)-C(15)-C(16)	114.5(4)	114.1(4)
C(15)-C(16)-N(2)	118.8(4)	118.2(4)
M-N(2)-C(16)	114.5(3)	114.4(3)
M-N(2)-C(17)	123.7(3)	125.7(3)
C(16)-N(2)-C(17)	120.6(4)	119.9(4)

^a G represents the centroids of the $\eta^5\text{-C}_5\text{Me}_5$ (**1a**) or the $\eta^6\text{-}p\text{-MeC}_6\text{H}_4\text{iPr}$ (**7b**) rings.

tures are compared, they only show remarkable differences in the η^n -ring coordination; thus, while the C_5Me_5 atoms are bonded to Rh with statistically equal bond distances (Rh-C range 2.154–2.173(5) Å), the Ru-C bond lengths of the $\eta^6\text{-}p\text{-MeC}_6\text{H}_4\text{iPr}$ ligand are spread over a large range (2.177–2.260(5) Å), probably reflecting the greater and asymmetric steric requirement of the respective imine ligands.

The chemical shift of the imine H_b protons appears at significantly higher field for compounds **1a**, **2a**, **4a,b**, and **5a,b** than for their corresponding epimers (primed labeling) but does not differ appreciably between the remaining pairs of epimers. This high-field shift of the H_b hydrogens seems to be a general behavior for substituted $\eta^n\text{-ring-Ir}^{\text{III}}$, Rh^{III} , or Ru^{II} half-sandwich compounds with imine ligands where aromatic substituents are bonded to the asymmetric imine carbon. It is most probably due to a ring current effect from these aromatic substituents. A plausible conformation around the asymmetric carbon atom of the imine for the unprimed isomers would be that depicted in Figure 3a. The aromatic substituent R approximately eclipses the N_{im}-C(H_b) bond when viewed through the C(asymmetric) to metal axis. This conformation would explain the shielding of the H_b proton if R is, additionally, face-on to the imine hydrogen. Furthermore, if the configuration at the metal is R , the proposed conformation places the smallest sized substituent on the asymmetric carbon atom of the imine, H_a, pointing toward the η^n -ring, which is the bulkiest substituent on the metal.

Remarkably, in the conformation adopted in the solid state, the H_b protons usually do not lie in the shielding cone of the aromatic substituent (see Figure 1). This is

(12) (a) Cahn, R. S.; Ingold, C.; Prelog, V. *Angew. Chem., Int. Ed. Engl.* **1966**, *5*, 385. (b) Lecomte, C.; Dusausoy, Y.; Protas, J.; Tirouflet, J. J. *Organomet. Chem.* **1974**, *73*, 67. (c) Stanley, K.; Baird, M. C. J. *Am. Chem. Soc.* **1975**, *97*, 6599. (d) Sloan, T. E. *Top. Stereochem.* **1981**, *12*, 1.

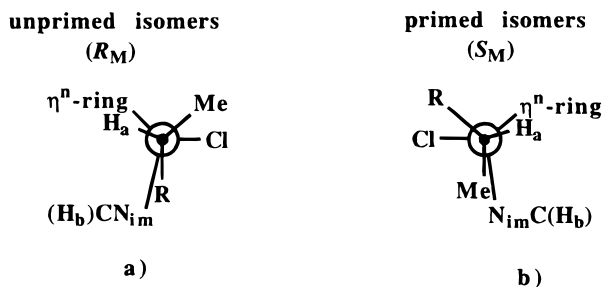


Figure 3. Schematic view along the C(imine)–M direction of the proposed conformations in (a) R_M or (b) S_M isomers.

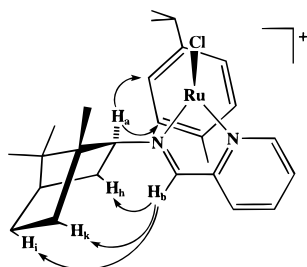


Figure 4. Schematic view of the cation of **7b**. Proton labeling and some selected NOE are shown.

also the case for the related iridium compounds⁸ (R_{Ir}, R_C)- $[(\eta^5\text{-C}_5\text{Me}_5)\text{IrCl}(\text{L}_n)][\text{SbF}_6]$ ($\text{L}_n = \text{L}_1, \text{L}_2, N\text{-}(2\text{-quinolylmethylene})\text{-}(R)\text{-}1\text{-naphthylethylamine}$). The stabilization of the solid state conformation may be due to an attractive interaction between the aromatic ring and one of the methyl groups of the C_5Me_5 ligand, a $\text{CH}_3 \cdots \pi$ interaction,¹³ closely related to the “ β -phenyl effect” reported by Brunner et al. in structurally comparable half-sandwich derivatives.^{4f} Supporting this proposal, the distances between the methyl carbon C(7) and the carbon atoms C(19), C(20), and C(21) of the phenyl substituent are 3.660(7), 3.596(7), and 3.987(10) Å, respectively. A similar situation is observed in the iridium homologues (R_{Ir}, R_C)- $[(\eta^5\text{-C}_5\text{Me}_5)\text{IrCl}(\text{L}_n)][\text{SbF}_6]$ ($\text{L}_n = \text{L}_1, \text{L}_2$, or $N\text{-}(2\text{-quinolylmethylene})\text{-}(R)\text{-}1\text{-naphthylethylamine}$) recently reported by us. (The corresponding methyl–C(aromatic) distances range from 3.386(8) to 4.029(11) Å).⁸ However, one of the two independent molecules found in the solid-state structure of the related mesitylene ruthenium compound (S_{Ru}, S_C)- $[(\eta^6\text{-mes})\text{RuCl}(\text{imine})]\text{BF}_4$ (imine = $N\text{-}(2\text{-pyridylmethylene})\text{-}(S)\text{-}1\text{-phenylethylamine}$) presents a conformation in which the phenyl substituent is almost eclipsed and face-on to the imine nitrogen.⁴ⁱ Thus, it can be concluded that the energy difference between these two conformations should be small and the observation of one of them depends on subtle effects.

It has been pointed out above that the single crystal of the ruthenium compound used in the X-ray diffractometric analysis was grown from a 90:10 **7b/7b'** molar ratio mixture of diastereomers. The ¹H NMR spectrum of the remaining single crystals also revealed a 90:10 molar ratio between the two components, and the X-ray analyzed crystal was the R_{Ru} epimer. Solution NOED-IFC spectra (Figure 4) of a diastereomerically pure sample of the major component showed that irradiation of the H_a proton led to enhancement of one of the two

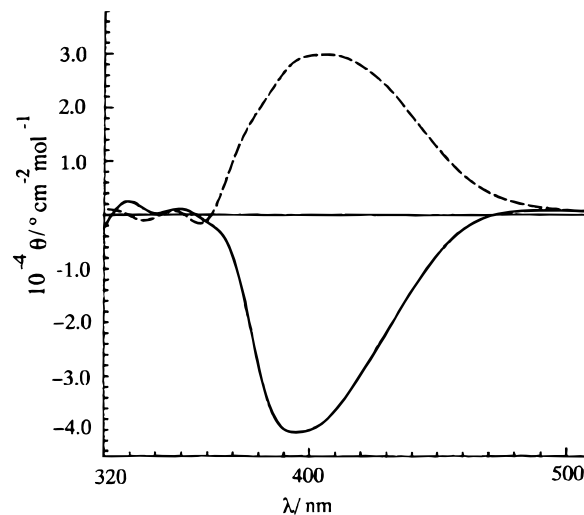


Figure 5. CD spectra (Me_2CO , $1.25 \times 10^{-3} \text{ mol L}^{-1}$) of complex **3a** (—) and of a 17:83 **3a/3a'** mixture (---).

AB spin systems of the aromatic $p\text{-MeC}_6\text{H}_4\text{Pr}$ protons (7.6 and 9.3%), indicating that the H_a proton is pointing toward the p -cymene group. It seems reasonable that the smallest sized H_a proton is close to the bulkiest $p\text{-MeC}_6\text{H}_4\text{Pr}$ ligand in both diastereomers. In fact, in the crystal, the dihedral angle $\text{G-Ru} \cdots \text{C}(17)\text{-H}(17)$ ¹⁴ is 0.8° . Additionally, irradiation of the H_b proton caused an enhancement of the H_h proton at $\delta = 1.92$ (14.7%) but also of H_i at $\delta = 1.54$ (7.7%) and H_k at $\delta = 1.36$ (4.7%).¹⁵ In good agreement with this, the calculated $\text{H}_b \cdots \text{H}_h$, $\text{H}_b \cdots \text{H}_i$, and $\text{H}_b \cdots \text{H}_k$ distances in the crystal structure are 1.918(1), 2.370(1), and 2.734(1) Å, respectively. All these data strongly suggest that the major component of the solution mixture should be the R_{Ru} epimer, the isomer characterized in the solid state.¹⁶

Circular Dichroism Spectra. To establish the configuration at the metal for both diastereomers, the circular dichroism (CD) spectra of complexes **1–7** were measured. The CD spectrum of a diastereomerically pure sample of the rhodium complex **1a** (R_{Rh} epimer) consists of a maximum with negative Cotton effect at ca. 400 nm. The CD spectra of a 70:30 **a/a'** mixture of **2** or enantiopure **3a** also show a negative Cotton effect, centered at 390 and 395 nm, respectively. As expected for epimers configurationally stable at the metal center (see below) which differ in the metal configuration, **a** and **a'** pairs exhibit CD spectra which are approximately mirror images of each other,^{2d,17} showing that the major contribution to the spectra corresponds to the metal chromophore. In fact, the CD spectra of the free imine ligands does not show any transition above 350 nm. As a representative example, Figure 5 shows the pseudo-enantiomorphous relationship between **3a** and a 17:83 **3a/3a'** mixture. The known R_{Rh} configuration of the epimer

(14) G represents the centroid of the $p\text{-MeC}_6\text{H}_4\text{Pr}$ ring.

(15) The assignment of the bornyl protons has been accomplished by COSY, NOESY, and selective proton decoupling experiments.

(16) The configuration at the ruthenium has been inverted by using computer-assisted molecular models. (*Chem3D: Molecular modeling and analysis*; Cambridge Soft Corporation: Cambridge, 1995.) The calculated $\text{H}_b \cdots \text{H}_h$, $\text{H}_b \cdots \text{H}_i$, and $\text{H}_b \cdots \text{H}_k$ distances are 3.575, 3.192, and 1.209 Å, respectively. Thus, in the S_{Ru} epimer, irradiation of the H_b proton would cause enhancement of the H_k hydrogen but smaller NOE effects on the H_i and H_h protons in opposition to the experimental results.

(17) Brunner, H. *Adv. Organomet. Chem.* **1980**, *18*, 151.

(13) Andreotti, G. D.; Ori, O.; Ugozzoli, F.; Alfieri, C.; Pochini, A.; Ungaro, R. *J. Inclusion Phenom.* **1988**, *6*, 523.

Table 3. Diastereomeric Compositions of Complexes 1–7

complex	initial R_M/S_M molar ratio	equilibrium R_M/S_M cation molar ratio
1	96:4	85:15
2	55:45	77:23
3	41:59	10:90
5	58:42	75:25
6	42:58	25:75
7	13:87	89:11

1a (X-ray analysis), along with the CD data, allows us to propose the R_{Rh} and S_{Rh} configurations for the **a** and **a'** isomers of the rhodium compounds **1–3**, respectively.

The CD spectrum of a 90:10 **7b/7b'** mixture shows a very strong negative Cotton effect centered at 470 nm. As stated above, the major component of the mixture exhibits the R_{Ru} configuration. The CD spectrum of a 15:85 **7b/7b'** mixture displays a pseudoenantiomeric relationship, consisting of a maximum with positive Cotton effect centered at 445 nm. Consistently, the CD spectra of mixtures of complexes **4–7** enriched in the unprimed component also show a maximum with negative Cotton effect, and vice versa. All these data allow us to propose the R or S configuration at ruthenium for isomers **4a,b–7a,b** or **4a',b'–7a',b'**, respectively.

Epimerization of the Complexes 1–7. At room temperature, in acetone or chloroform solution, the metal center in complexes **1–7** is configurationally stable; the composition of solution mixtures of epimers remains unchanged for days. This configurational stability is comparable to that found in the related iridium compounds⁸ $[(\eta^5\text{-C}_5\text{Me}_5)\text{IrCl}(\text{L}_n)][\text{SbF}_6]$ and strongly contrasts with the high lability found for related half-sandwich iridium, rhodium, or ruthenium systems with imino^{4d,e,h} or amino acidato^{7a,b,18} N,O ligands. However, at higher temperatures, in more polar solvents such as methanol, the complex cations slowly epimerize at the metal center, with no apparent decomposition. Only the cation of complex **4** partially decomposes under these conditions. Table 3 collects the initial diastereomeric compositions¹¹ and those at the equilibrium reached after about 30 h of treatment in refluxing methanol. The latter composition remains unchanged after refluxing the mixtures for an additional 8 h.

The thermodynamically more stable diastereomer is the R epimer for those complexes containing the imines L_1 , L_2 , or L_4 but the S epimer for complexes **3** and **6** containing the L_3 ligand. Figure 3 shows a schematic view of the projection of the R_M and S_M isomers along the C(asymmetric)–M axis. Assuming that the H_a proton points to the η^n -ring ligand in both diastereomers, the R substituent and the essentially planar IrNCCN metallacycle (represented in Figure 3 by the $N_{\text{im}}\text{C}(H_b)$ group) should be in almost eclipsing positions in the R_M isomer. This conformation is favored with respect to that adopted by the S_M isomers (obtained by interchanging the relative positions of the Me and R groups) when R is the planar phenyl or naphthyl substituent. However, when R is the nonplanar cyclohexyl group (complexes **3** and **6**), there should be an important repulsive interaction, in the R_M epimers, between the axial protons of this group and the $N_{\text{im}}\text{C}$

(H_b) moiety, thus favoring the S_M isomers. NOEDIFF experiments support this proposal. While irradiation of the H_b proton of **3a** produces enhancement of some of the cyclohexyl protons (12.2%), no enhancement of the corresponding cyclohexyl protons is observed when the H_b proton of **3a'** is irradiated. Moreover, irradiation of H_b in **3** produces a slightly greater enhancement of the Me group of the chiral imine in **3a'** (4.9%) than for that in **3a** (4.1%). Similar results have previously been reported for the $(\eta^5\text{-C}_5\text{Me}_5)\text{Ir}$ homologues of **3** and **6**.⁸

Catalytic Diels–Alder Reactions. To confirm the ability of the chiral half-sandwich imine systems as enantioselective Diels–Alder catalysts, we attempted the preparation of solvate complexes from the above-reported chloro compounds. Thus, treatment of dichloromethane solutions of **1–7** with equimolar amounts of the corresponding silver salt AgA ($A = \text{SbF}_6$ or BF_4) in a minimum amount of acetone¹⁹ afford compounds of general formula $[(\eta^n\text{-ring})\text{M}(\text{imine})\text{S}]\text{A}_2$. NMR spectroscopic measurements reveal that the solids consist of mixtures of epimers at the metal center with different solvate ligands. Similar results are obtained by reacting the dimer $\{[(\eta^5\text{-C}_5\text{Me}_5)\text{RhCl}]_2(\mu\text{-Cl})_2\}$ with AgSbF_6 in methanol and subsequent addition of 1 equiv of the imine L_1 to the resulting solvate²⁰ $[(\eta^5\text{-C}_5\text{Me}_5)\text{Rh}(\text{MeOH})_3]^{2+}$.

The major component of the mixtures is, most probably, the aquo complexes $[(\eta^n\text{-ring})\text{M}(\text{imine})(\text{H}_2\text{O})]^{2+}$, with the coordinated water coming from adventitious water of the organic solvent. The rhodium aquo complexes are fluxional on the NMR time scale. At room temperature, in acetone- d_6 , the ^1H NMR spectra of the aquo complexes prepared from compounds **1** and **2** consists of a set of broad signals, whereas at -80°C two sets of peaks are observed in 70:30 intensity ratio. For the ruthenium compounds, the mixtures contain comparable amounts of at least three components whose structures were not further investigated.

The in situ generated solvates were used as catalysts for the Diels–Alder reaction between methacrolein or acrolein and cyclopentadiene. Tables 4 and 5 collect some of the catalytic experiments with methacrolein or acrolein, respectively. At room temperature, both reactions are effectively catalyzed by the solvates at low catalyst loading (5% mol) with good exo/endo (methacrolein) or endo/exo (acrolein) selectivities but without enantioselection. Only modest inductions (from 10 to 21%) are obtained, at low temperature, for the acrolein reaction by using complex **3** as the precursor (entries 13–15, Table 5). Lowering the reaction temperature (Table 4, entries 8 and 9; Table 5, entries 7 and 8) or using acetone as the solvent (Table 4, entries 10 and 11; Table 5, entries 9 and 10) gives a reduction in the reaction rate as the sole detectable effect. The BF_4^- salts (Table 4, entries 12 and 13; Table 5, entries 11 and 12) behave similarly to the SbF_6^- salts, despite the fact that large improvements in both rate and enantioselectivity have been associated with changes in the counteranion.^{3d,21} Finally, the use as precatalysts of the S_M

(19) The AgA salts are not soluble enough in dichloromethane to cause precipitation of silver chloride from compounds **1–7**.

(20) White, C.; Thompson, S. J.; Maitlis, P. M. *J. Chem. Soc., Dalton Trans.* **1977**, 1654.

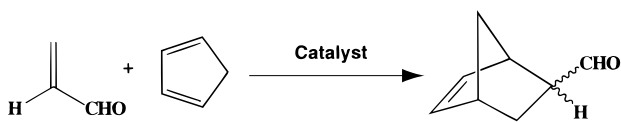
(21) Evans, D. A.; Murry, J. A.; von Matt, P.; Norcross, R. D.; Miller, S. J. *Angew. Chem., Int. Ed. Engl.* **1995**, *34*, 798.

(18) Krämer, R.; Polborn, K.; Wanjek, H.; Zahn, I.; Beck, W. *Chem. Ber.* **1990**, *123*, 767.

Table 4. Catalytic Diels–Alder Reaction of Methacrolein with Cyclopentadiene

entry	precatalyst (R_M/S_M , ratio)	solvent ^a	temp (°C)	time (h)	yield (%)	isomer ratio (exo/endo)	ee ^b (%)
1		CH ₂ Cl ₂	RT	1	0.5		
2	1a,a' (96:4)	CH ₂ Cl ₂	RT	1.2	76	85:15	0
3	3a,a' (>98:<2)	CH ₂ Cl ₂	RT	0.4	75	82:18	0
4	4a,a' (65:35)	CH ₂ Cl ₂	RT	1.3	94	84:16	0
5	5a,a' (63:37)	CH ₂ Cl ₂	RT	1.8	67	86:14	4 (S)
6	6a,a' (58:42)	CH ₂ Cl ₂	RT	0.6	95	82:18	5 (S)
7	7a,a' (44:56)	CH ₂ Cl ₂	RT	17	80	83:17	0
8	1a,a' (96:4)	CH ₂ Cl ₂	-20	96	78	86:14	0
9	6a,a' (58:42)	CH ₂ Cl ₂	-20	112	91	87:13	5 (R)
10	3a,a' (>98:<2)	Me ₂ CO	RT	71	72	93:7	8 (S)
11	7a,a' (44:56)	Me ₂ CO	RT	174	32	86:14	0
12	6b,b' (58:42)	CH ₂ Cl ₂	RT	0.9	82	83:17	3 (R)
13	4b,b' (65:35)	CH ₂ Cl ₂	RT	1.3	94	84:16	0
14	3a,a' (17:83)	CH ₂ Cl ₂	RT	1.25	71	91:9	0
15	3a,a' (17:83)	Me ₂ CO	RT	72	43	92:8	3 (S)

^a Catalytic CH₂Cl₂ solutions contained ca. 9% (v/v) of Me₂CO (see text). ^b Absolute configuration at C₂.

Table 5. Catalytic Diels–Alder Reaction of Acrolein with Cyclopentadiene

entry	precatalyst (R_M/S_M , ratio)	solvent ^a	temp (°C)	time (h)	yield (%)	isomer ratio (endo/exo)	ee ^b (%)
1		CH ₂ Cl ₂	RT	0.5	15	79:21	
2	1a,a' (96:4)	CH ₂ Cl ₂	RT	0.4	74	84:16	0
3	4a,a' (65:35)	CH ₂ Cl ₂	RT	0.3	99	80:20	5 (R)
4	5a,a' (63:37)	CH ₂ Cl ₂	RT	0.3	81	81:19	3 (R)
5	6a,a' (58:42)	CH ₂ Cl ₂	RT	0.7	94	88:12	3 (S)
6	7a,a' (44:56)	CH ₂ Cl ₂	RT	8	84	78:22	0
7	4a,a' (65:35)	CH ₂ Cl ₂	-20	2.4	97	82:18	5 (S)
8	6a,a' (58:42)	CH ₂ Cl ₂	-20	52	89	82:18	3 (S)
9	5a,a' (63:37)	Me ₂ CO	RT	22	97	80:20	5 (S)
10	6a,a' (58:42)	Me ₂ CO	RT	8	98	84:16	3 (S)
11	4b,b' (65:35)	CH ₂ Cl ₂	RT	0.9	80	86:14	2 (S)
12	6b,b' (58:42)	CH ₂ Cl ₂	RT	0.7	84	88:12	0
13	3a,a' (>98:<2)	CH ₂ Cl ₂	-20	4.2	96	80:20	10 (S)
14	3a,a' (17:83)	CH ₂ Cl ₂	-20	4.4	85	72:28	16 (S)
15	3a,a' (17:83)	CH ₂ Cl ₂	-50	22	73	73:27	21 (S)
16	3a,a' (17:83)	Me ₂ CO	RT	6.2	68	77:23	8 (S)

^a Catalytic CH₂Cl₂ solutions contained ca. 9% (v/v) of Me₂CO (see text). ^b Absolute configuration at C₂ for the endo isomer.

epimer instead of the R_M epimer (Table 4, entries 14 and 15) does not significantly alter the catalytic results.

Experimental Section

General Comments. All solvents were distilled under nitrogen and degassed prior to being used. All preparations were carried out under a nitrogen atmosphere. Infrared spectra were recorded on a Perkin-Elmer 783 spectrophotometer. Carbon, hydrogen, and nitrogen analyses were performed using a Perkin-Elmer 240B microanalyzer. ¹H NMR spectra were recorded on a Varian UNITY 300 (299.95 MHz) or a Bruker 300 ARX (300.10 MHz) spectrometer. Chemical shifts are expressed in ppm relative to SiMe₄. The probe temperature was calibrated against a methanol standard. COSY and NOESY NMR spectra were obtained using standard procedures. CD spectra were determined in Me₂CO (ca. 10⁻³ mol L⁻¹ solutions) in a 1 cm path length cell by using a Jasco-710 apparatus.

Preparation of [(η^5 -C₅Me₅)RhCl(imine)]SbF₆ (1–3). A mixture of [(η^5 -C₅Me₅)RhCl]₂(μ -Cl)₂ (0.65 mmol), NaSbF₆ (1.30 mmol), and the appropriate imine ligand (1.30 mmol) was stirred in methanol (25 mL) for 1 h. During this time the precipitation of a yellow solid was observed. The mixture was subsequently filtered, and the filtrate was evaporated to dryness. The resulting solid was extracted with dichloromethane (15 mL), and this solution was partially concentrated under reduced pressure. Slow addition of diethyl ether gave an orange microcrystalline solid, which was isolated by filtration, washed with diethyl ether, and air-dried. Complex **1**. Yield: first fraction, 61%, **1a/1a'** molar ratio, 97:3; second fraction, 28%, **1a/1a'** molar ratio, 95:5. Anal. Calcd for C₂₄H₂₉N₂-ClF₆RhSb: C, 40.0; H, 4.0; N, 3.9. Found: C, 40.05; H, 4.1; N, 3.9. IR (Nujol, cm⁻¹): ν (CN) 1600 (m), ν (SbF₆) 285 (s). Complex **2**. Yield: first fraction, 68%, **2a/2a'** molar ratio, 50:50; second fraction, 24%, **2a/2a'** molar ratio, 70:30. Anal. Calcd for C₂₈H₃₁N₂ClF₆RhSb: C, 43.7; H, 4.0; N, 3.6. Found: C, 43.4; H, 4.1; N, 3.6. IR (Nujol, cm⁻¹): ν (CN) 1595 (m), ν (SbF₆) 290 (s). Complex **3**. Yield: first fraction, 27%, **3a/3a'** molar ratio, >98:<2; second fraction, 66%, **3a/3a'** molar ratio, 17:83. Anal. Calcd for C₂₄H₃₅N₂ClF₆RhSb: C, 39.7; H, 4.8; N, 3.9. Found: C, 40.1; H, 4.4; N, 3.8. IR (Nujol, cm⁻¹): ν (CN) 1600 (m), ν (SbF₆) 285 (s).

Preparation of [(η^6 -*p*-MeC₆H₄ⁱPr)RuCl(imine)]A (4a–7a and 4b–6b). A mixture of [(η^6 -MeC₆H₄ⁱPr)RuCl]₂(μ -Cl)₂ (0.25 mmol), NaSbF₆, or NaBF₄ (0.50 mmol) and the appropriate imine ligand (0.50 mmol) was stirred in methanol (25 mL) for 1 h. During this time, the color of the solution changed from orange to brown. The solvent was evaporated to dryness. The resulting solid was extracted with dichloromethane (15 mL), and this solution was partially concentrated under reduced pressure. Slow addition of diethyl ether gave an orange microcrystalline solid, which was isolated by filtration, washed with diethyl ether, and air-dried. Complex **4**. Yield: 78%, **4a/4a'** molar ratio, 65:35. Anal. Calcd for C₂₄H₂₈N₂ClF₆-RuSb: C, 40.2; H, 3.9; N, 3.9. Found: C, 39.9; H, 3.8; N, 3.7. IR (Nujol, cm⁻¹): ν (CN) 1596 (s), ν (SbF₆) 290 (m). Yield: 94%, **4b/4b'** molar ratio, 65:35. Anal. Calcd for C₂₄H₂₈N₂BClF₄Ru: C, 50.8; H, 5.2; N, 4.5. Found: C, 50.5; H, 5.1; N, 4.5. IR (Nujol, cm⁻¹): ν (CN) 1596 (s), ν (BF₄) 1059 (vs), 520 (s). Complex **5**. Yield: 81%, **5a/5a'** molar ratio, 63:37. Anal. Calcd for C₂₈H₃₀N₂-ClF₆RuSb: C, 43.9; H, 3.9; N, 3.6. Found: C, 43.7; H, 3.8; N, 3.7. IR (Nujol, cm⁻¹): ν (CN) 1597 (s), ν (SbF₆) 280 (m). Yield: 86%, **5b/5b'** molar ratio, 58:42. Anal. Calcd for C₂₈H₃₀N₂BClF₄-Ru: C, 54.4; H, 4.9; N, 4.5. Found: C, 54.4; H, 5.0; N, 4.5. IR (Nujol, cm⁻¹): ν (CN) 1598 (s), ν (BF₄) 1071 (vs), 525 (s). Complex **6**. Yield: 74%, **6a/6a'** molar ratio, 42:58. Anal. Calcd for C₂₄H₃₄N₂ClF₆RuSb: C, 39.9; H, 4.7; N, 3.9. Found: C, 39.6; H, 4.5; N, 3.8. IR (Nujol, cm⁻¹): ν (CN) 1595 (s), ν (SbF₆) 289 (m). Yield: 88%, **6b/6b'** molar ratio, 42:58. Anal. Calcd for C₂₄H₃₄N₂BClF₄Ru: C, 50.2; H, 6.0; N, 4.9. Found: C, 49.9; H, 5.7; N, 4.8. IR (Nujol, cm⁻¹): ν (CN) 1595 (s), ν (BF₄) 1064 (vs), 524 (s). Complex **7**. Yield: 77%, **7a/7a'** molar ratio, 44:56. Anal. Calcd for C₂₆H₃₆N₂ClF₆RuSb: C, 41.7; H, 4.8; N, 3.7. Found: C, 41.4; H, 4.8; N, 3.6. IR (Nujol, cm⁻¹): ν (CN) 1593 (s), ν (SbF₆) 290 (m).

Preparation of [(η^6 -*p*-MeC₆H₄ⁱPr)RuClL₂][BF₄] (7b,b'). A mixture of [(η^6 -MeC₆H₄ⁱPr)RuCl]₂(μ -Cl)₂ (200.0 mg, 0.33 mmol), NaBF₄ (72.5 mg, 0.66 mmol), and 73.1 mg (0.66 mmol) of *N*-(2-pyridylmethyl)-(*1R,2S,4R*)-1-bornylamine was stirred in methanol (25 mL) for 1 h. During this time, the color of the solution changed from orange to red. Partial evaporation of the solvent gave the precipitation of an orange solid which was isolated by filtration, washed with cold methanol, and air-dried. Further concentration of the filtrate produced a second crop of the orange product which was isolated in a similar manner. The remaining filtrate was evaporated to dryness, and the residue was extracted with dichloromethane (15 mL). The resulting solution was partially concentrated under reduced pressure. Slow addition of diethyl ether gave an

orange microcrystalline solid, which was isolated by filtration, washed with diethyl ether, and air-dried. Yield: first fraction, 33%, **7b/7b'** molar ratio, 90:10; second fraction, 19%, **7b/7b'** molar ratio, 50:50; third fraction, 31%, **7b/7b'** molar ratio, 13:87. Anal. Calcd for $C_{26}H_{36}N_2BClF_4Ru$: C, 52.1; H, 6.0; N, 4.7. Found: C, 51.9; H, 5.8; N, 4.6. IR (Nujol, cm^{-1}): $\nu(CN)$ 1593 (s), $\nu(BF_4)$ 1058 (vs), 520 (s).

Catalytic Diels–Alder Reaction between Methacrolein or Acrolein and Cyclopentadiene. The corresponding precatalyst **1–7** (0.025 mmol) in acetone/dichloromethane (0.2/2 mL) was treated with the appropriate silver salt (0.025 mmol), and the resulting suspension was stirred for 15 min. After this time, the AgCl was removed by filtration through Celite. The filtrate was kept under argon at the appropriate reaction temperature. The dienophile (0.5 mmol in 2 mL of CH_2Cl_2) and freshly distilled cyclopentadiene (3 mmol in 2 mL of CH_2Cl_2) were then added by syringe. The resulting solution was stirred at the reaction temperature and monitored by gas chromatography (GC). The yield and exo/endo ratio were determined by GC. The reaction mixture was concentrated to ca. 0.3 mL and filtered through silica gel, washing with CH_2Cl_2/n -hexane (1/3) before the determination of the enantiomeric purity. Ee's were determined by integration of the aldehyde proton of both enantiomers using $Eu(hfc)_3$ as a chemical shift reagent ($Eu(hfc)_3$ /adduct ratio, 0.3). The absolute configuration of the major adduct was assigned by comparing the sign of $[\alpha]_D$ with that of the literature.²²

Crystal Structure Determination of Complexes 1a and 7b. A summary of crystal data, intensity collection, and refinement parameters for the two structural analyses is reported in Table 6. The orange crystals used for the X-ray analysis were glued to glass fibers and mounted on a Siemens-Stoe AED-2 (**1a**) or on a Siemens P4 diffractometer (**7b**) and irradiated with graphite-monochromated Mo $K\alpha$ radiation ($\lambda = 0.71073 \text{ \AA}$). Cell constants were obtained from the least-squares fit on the setting angles of 52 reflections ($25 \leq 2\theta \leq 35^\circ$) for **1a** or 68 ($25 \leq 2\theta \leq 38^\circ$) for **7b**. For both crystals, a complete set of independent reflections with 2θ up to 55° were measured at 200 K using the $\omega/2\theta$ scan technique and subsequently corrected for Lorentz and polarization effects. Reflections were also corrected for absorption by a semiempirical method (Ψ -scan).²³ Three standard reflections were monitored (every 60 min of measuring time (**1a**) or every 100 measurements (**7b**)) throughout data collection as a check on crystal and instrument stability; a weak decay observed for **1a** (1.24%) was corrected according to standard reflections.

Both structures were solved by direct methods and subsequent difference Fourier techniques (SHELXTL-PLUS)²⁴ and refined by full-matrix least-squares on F^2 (SHELXL-97).²⁵ In the crystal structure of **7b**, the BF_4^- counteranions were observed to be statically disordered. They were modeled with two different BF_4 moieties refined with feeble geometrical restraints (DFIX applied to B–F and F...F distances) and

Table 6. Crystal Data and Data Collection and Refinement for 1a and 7b

	1a	7b
chem formula	$C_{24}H_{29}ClF_6N_2RhSb$	$C_{26}H_{36}BClF_4N_2Ru$
fw	719.60	599.90
crystal size, mm	$0.72 \times 0.46 \times 0.19$	$0.26 \times 0.20 \times 0.09$
space group	$P2_1$ (no. 4)	$P2_1$ (no. 4)
<i>a</i> , Å	8.3211(8)	8.0547(13)
<i>b</i> , Å	10.4917(15)	18.164(3)
<i>c</i> , Å	15.835(2)	9.8878(16)
β , deg	100.497(12)	111.259(9)
<i>V</i> , Å ³	1359.3(3)	1348.2(5)
<i>Z</i>	2	2
D_{calcd} , g cm ⁻³	1.758	1.478
μ , mm ⁻¹	1.755	0.726
no. of measd reflns	7220 ($2\theta \leq 55^\circ$)	15710 ($2\theta \leq 55^\circ$)
no. of unique reflns	6256 ($R_{\text{int}} = 0.0559$)	6183 ($R_{\text{int}} = 0.0068$)
min, max trasm fact ^a	0.364, 0.732	0.841, 0.903
no. data/restraints/ params	6256/1/326	6183/21/324
$R(F)$ ($F^2 \geq 2\sigma(F^2)$) ^b	0.0391	0.0447
$wR(F^2)$ (all data) ^c	0.1032	0.0836

^a A semiempirical ψ -scan absorption correction was applied. ^b $R(F) = \sum ||F_o| - |F_c|| / \sum |F_o|$ for 6106 (**1a**) and 5307 (**7b**) observed reflections. ^c $wR(F^2) = [\sum [w(F_o^2 - F_c^2)^2] / \sum [w(F_o^2)^2]]^{1/2}$; $w^{-1} = [\sigma^2(F_o^2) + (aP)^2 + bP]$, where $P = [\max(F_o^2, 0) + 2F_c^2]/3$ (**1a**: $a = 0.0768$, $b = 0.8063$; **7b**: $a = 0.0068$; $b = 3.2679$).

complementary occupancy factors. Anisotropic thermal parameters were used in the last cycles of refinement for all non-hydrogen atoms except the fluoride atoms of the anionic BF_4^- groups involved in the disorder (**7b**). The hydrogen atoms of the terminal methyl groups were placed at their calculated positions; the positions of the remaining ones were obtained from difference Fourier maps. All were refined riding on carbon atoms with three (**1a**) or four (**7b**) common isotropic displacement parameters. The function minimized was $\sum [w(F_o^2 - F_c^2)^2]$. The calculated weighting scheme was $1/[\sigma^2(F_o^2) + (aP)^2 + bP]$, where $P = [\max(F_o^2, 0) + 2F_c^2]/3$. All the refinements converged to reasonable *R* factors (Table 6). The absolute structure has been checked in both structures by the estimation of the Flack parameter *x* in the final cycles of refinement, $-0.05(3)$ (**1a**) and $-0.04(4)$ (**7b**).²⁶ The highest residual electron density peaks, of 1.40 (**1a**) and 0.59 (**7b**) e/Å³, were situated in close proximity to the metal centers and have no chemical sense. Scattering factors were used as implemented in the refinement program.²⁵

Acknowledgment. We thank the Dirección General de Investigación Científica y Técnica for financial support (Grant PB96/0845). S.E. thanks the DGICYT for a grant.

Supporting Information Available: Full listings of crystallographic data, complete atomic coordinates, isotropic and anisotropic thermal parameters, and bond distances and angles for complexes **1a** and **7b** (CIF format). This material is available free of charge via the Internet at <http://pubs.acs.org>.

OM9810448

(26) Flack, H. D. *Acta Crystallogr.* **1983**, *A39*, 876.

(22) Furuta, K.; Shimizu, S.; Miwa, Y.; Yamamoto, H. *J. Org. Chem.* **1989**, *54*, 1481.

(23) North, A. C. T.; Phillips, D. C.; Mathews, F. S. *Acta Crystallogr.* **1968**, *A24*, 351.

(24) Sheldrick, G. M. *SHELXTL-PLUS*; Siemens Analytical X-ray Instruments: Madison, WI, 1990.

(25) Sheldrick, G. M. *SHELXL-97 Program for Crystal Structure Refinement*; University of Göttingen: Göttingen, Germany, 1997.